

MIT Open Access Articles

The Case for Parameter-Aware Control of Assistive Free-Flyers

The MIT Faculty has made this article openly available. **Please share** how this access benefits you. Your story matters.

Citation: Albee, Keenan and Cabrales Hernandez, Alejandro d. 2021. "The Case for Parameter-Aware Control of Assistive Free-Flyers." AIAA SciTech Forum.

As Published: 10.2514/6.2021-2018

Publisher: American Institute of Aeronautics and Astronautics

Persistent URL: <https://hdl.handle.net/1721.1/142474>

Version: Author's final manuscript: final author's manuscript post peer review, without publisher's formatting or copy editing

Terms of use: Attribution-NonCommercial-ShareAlike 4.0 International





The Case for Parameter-Aware Control of Assistive Free-Flyers

Keenan Albee[†] and Alejandro Cabrales Hernandez[†]
Massachusetts Institute of Technology, Cambridge, MA 02139

Manipulator-equipped microgravity robots (free-flyers) have been proposed for on-orbit activities including assisting astronauts with daily tasks and serving as mobile workers in microgravity assembly scenarios. An emerging class of free-flyer, assistive free-flyers (AFFs), will engage in complex manipulation scenarios such as grasping and moving new objects. This introduces a notable source of uncertainty in the form of inertial parametric uncertainty stemming from grappling unknown or poorly-characterized objects. This paper explicitly demonstrates the value—and perhaps even necessity—of control that can account for parametric uncertainty in these AFF manipulation scenarios, which involve more agile motion and larger end effector mass fractions than more traditional on-orbit free-flyer control situations. In this case study, a six degree of freedom base AFF with a two-link manipulator grapples an unknown point mass. The free-flying manipulator dynamics are detailed and a complex feasible reference trajectory, representative of those potentially seen by future AFFs, is provided. Two non-adaptive controllers, proportional-derivative (PD) and feedback linearization, are compared with sliding mode adaptive control for varying grappled mass fraction. A Lyapunov-based convergence analysis of the adaptive controller is also explicitly provided. Drawing from the prior free-flying literature, the value of parameter-aware control design for emerging AFF control scenarios is demonstrated.

I. Nomenclature

\mathbf{a}	=	uncertain parameter vector
\mathbf{C}	=	Coriolis matrix of manipulator equations
\mathbf{H}	=	inertia matrix of manipulator equations
\mathbf{q}	=	joint vector
\mathbf{q}_0	=	base orientation vector
\mathbf{r}	=	position/angle state vector
\mathbf{r}_0	=	base position vector
\mathbf{s}	=	sliding variable vector
\mathbf{v}	=	velocity state vector
\mathbf{x}	=	state vector
\mathbf{x}_{des}	=	desired reference state vector
\mathbf{Y}	=	system parameterization vector
$\boldsymbol{\tau}$	=	generalized force vector

II. Introduction

Interest in microgravity free-flyers (mobile satellite platforms that operate using both thrusters and internal reconfiguration like a manipulator arm) has grown as small satellites and on-orbit testbeds proliferate [1] [2]. These free-flyers, whose dynamics were extensively analyzed by Dubowsky and others in the late 1980s and early 1990s, are now of interest for a broader array of scenarios including active debris removal, on-orbit servicing, on-orbit assembly, and close-proximity astronaut assistance [3] [4]. These new mission scenarios often involve agile trajectory planning and control and large end effector mass fractions. The systems performing these missions are termed assistive free-flyers (AFFs).

[†]Ph.D. Student, Space Systems Laboratory, Department of Aeronautics and Astronautics, Massachusetts Institute of Technology. {albee, cabrales}@mit.edu

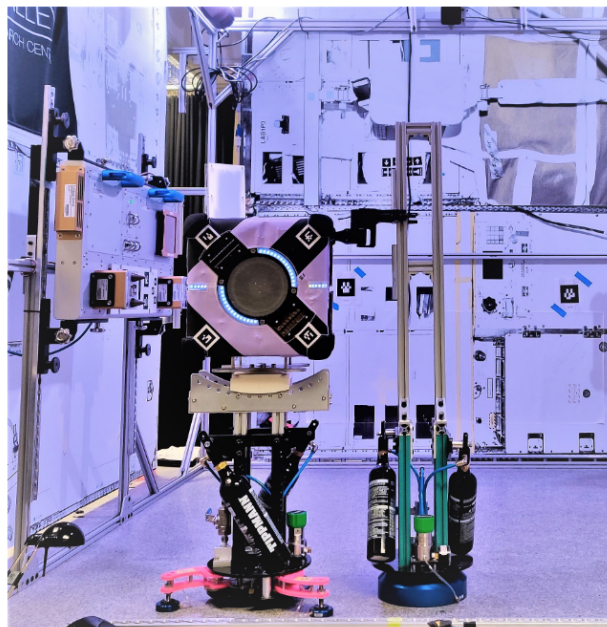


Fig. 1 The Astrobee Free-Flyer. NASA Ames’ Astrobee free-flyer, recently deployed to the ISS, is pictured here in its ground testbed with its robotic manipulator deployed grasping a large object. With a two-link robotic manipulator, Astrobee is first of its kind for on-orbit reusable testbeds exhibiting the free-flying manipulator dynamics. Credit: Monica Ekal.

AFFs are now emerging as a viable platform for astronaut assistance, on-orbit logistics automation, and bringing general-purpose robotics to the space domain. Astrobee, one of first practical deployments of an AFF shown in Fig. 1 [5] [6], has been operating on the International Space Station since early 2020 for instance. A useful scenario to consider for AFFs is the control problem after grappling a new, uncertain object. For example, after grappling a tool an AFF must now move under a modified set of system dynamics where the mass, center of mass location, and moment of inertia of the end effector linkage have potentially shifted. Yet, there is still little literature on planning and control scenarios relevant for these systems, and often no discussion of nonlinear control, particularly nonlinear control under parameter uncertainty.

Naturally, unknown constant system parameters invite the use of adaptive control as a solution to obtain better tracking performance. This problem has parallels to the adaptive control of fixed robotic manipulators, but with additional dynamics complexity from the free-flying base link; accordingly, a large amount of free-flying literature was developed beginning in the early 1990s detailing control approaches, primarily motivated by traditional on-orbit servicing scenarios. Fortunately, it has been demonstrated that essentially any control methodology for fixed-based manipulators can be used for free-floating (and free-flying) manipulators [7]. A variety of early methods were developed in the 1990s to control such systems [8], including a few adaptive controllers under varying assumptions (such as an attitude-controlled base) [9] [10] [11] [12]. A large portion of this research focused on the free-floating case, when base thrusters are not in use. Senda et al. later described a general purpose affine parameterization of inertial parameters that allows for the use of sliding mode adaptive control for general-purpose free-flying control [13]—this parameterization is not possible for free-floating control [9]. A variety of applications and modifications followed these early works, normally describing increasingly more complex systems and accounting for additional forms of uncertainty [14] [15] [16].

However, the vast majority of the literature focuses on a more traditional desired use case of on-orbit servicing, often only with two degree of freedom (DoF) base simulations with slow desired base motion, or without base motion. Further, when adaptive control is considered comparisons are infrequently made to more traditional control approaches and discussion of thrusters-on free-flying control is sometimes ignored. Bridging the gap between the healthy literature on this subject from earlier on-orbit servicing motivations, this paper aims to show a more AFF-relevant case study, provide an explicit comparison to other common controllers, and encourage discussion of the applicability of control techniques

accounting for parametric uncertainty to this emerging class of space system. This paper is organized as follows: the *Problem Formulation* introduces the general free-flying AFF dynamics and states the parametric uncertainty that arises; the *Approach* details three control methods, including an adaptive control method and its Lyapunov convergence analysis; the *Results* compare these control methods using multiple reference trajectories and show the adaptation properties of the adaptive controller; finally, the *Conclusion* comments on the need for parameter-aware control for AFFs and interesting future directions.

III. Problem Formulation

The formulation here largely follows from Dubowsky et al. and from Virgili-Llop et al. [3] [17]. There exists a free-flying space manipulator whose base is not rigidly fixed, resulting in a coupling between motion of the joints and motion of the base. In this case, a two-link manipulator operating with a six DoF base will be considered.

Fig. 2 is a representation of the free-flying manipulator system. The base, with corresponding frame ${}^0\mathcal{F}$, has a position ${}^I\mathbf{r}_0$ and orientation with respect to ${}^I\mathcal{F}$ of ${}^I_0\mathbf{q}_0$, with corresponding velocities ${}^I\dot{\mathbf{r}}_0$ and ${}^0\omega_0$, respectively. (Note that left superscripts for these quantities indicate their frame.) The joints of this particular manipulator are all revolute and oriented parallel to one another, so angular position for each joint is simply a scalar quantity. The vector of joint angles is given by ${}^0\mathbf{q}$, with corresponding joint rates ${}^0\dot{\mathbf{q}}$.

The system position, velocity, and state vectors may be written:

$$\mathbf{r} = \begin{bmatrix} {}^I\mathbf{r}_0^\top & {}^I_0\mathbf{q}_0^\top & {}^0\mathbf{q}^\top \end{bmatrix}^\top \quad (1)$$

$$\mathbf{v} = \begin{bmatrix} {}^I\dot{\mathbf{r}}_0^\top & {}^0\omega_0^\top & {}^0\dot{\mathbf{q}}^\top \end{bmatrix}^\top \quad (2)$$

$$\mathbf{x} = \begin{bmatrix} \mathbf{r}^\top & \mathbf{v}^\top \end{bmatrix}^\top \quad (3)$$

Using an XYZ body-fixed Euler angle parameterization, the full position and velocity vectors may be written:

$$\mathbf{r} = \begin{bmatrix} r_x & r_y & r_z & q_{0,x} & q_{0,y} & q_{0,z} & q_1 & q_2 \end{bmatrix}^\top \quad (4)$$

$$\mathbf{v} = \begin{bmatrix} \dot{r}_x & \dot{r}_y & \dot{r}_z & \omega_{0,x} & \omega_{0,y} & \omega_{0,z} & \dot{q}_1 & \dot{q}_2 \end{bmatrix}^\top \quad (5)$$

Note that a three DoF system simply disregards motion in the ${}^I\hat{\mathbf{z}}$ direction and rotation about the ${}^0\hat{\mathbf{x}}$ and ${}^0\hat{\mathbf{y}}$ axes—these terms may simply be set to zero if desired.

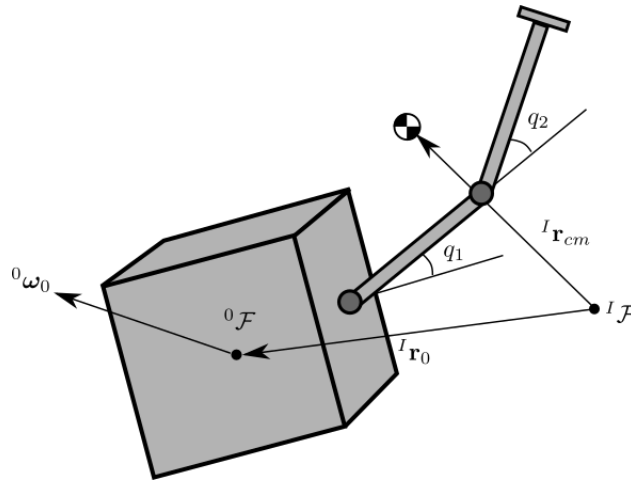


Fig. 2 System Sketch of a Two-Link Free-Flying Manipulator. The base is free to translate and rotate, resulting in a coupling between base and manipulator motion that is apparent in the manipulator equations.

The base and the links have masses $\{m_0, \dots, m_n\}$ and inertia tensors $\{\mathbf{I}_0, \dots, \mathbf{I}_n\}$, in addition to center of mass (CM) positions $\{\mathbf{r}_{CM,0}, \dots, \mathbf{r}_{CM,n}\}$. Geometrically, the links have joint-to-joint lengths $\{l_1, \dots, l_n\}$, with an initial manipulator offset \mathbf{l}_0 from the base CM.

The dynamics, presented in manipulator equation form in equation 6, are given by Dubowsky et al. using a Lagrangian derivation [3]. The version presented here also includes base translational motion and is presented relative to the base frame, with frame superscripts dropped for brevity:

$$\mathbf{H}(\mathbf{q})\dot{\mathbf{v}} + \mathbf{C}(\mathbf{q}, \omega_0, \dot{\mathbf{q}})\mathbf{v} = \boldsymbol{\tau} \quad (6)$$

Above, \mathbf{H} is the inertia matrix, \mathbf{C} is the matrix containing nonlinear terms (e.g., Coriolis), and $\boldsymbol{\tau}$ is the control vector. The control vector consists of the following forces and torques:

$$\boldsymbol{\tau} = \begin{bmatrix} {}^0\mathbf{F}_0^\top & {}^0\boldsymbol{\tau}_0^\top & {}^0\boldsymbol{\tau}_q^\top \end{bmatrix}^\top \quad (7)$$

$$\boldsymbol{\tau} = \begin{bmatrix} F_x & F_y & F_z & \tau_{0,x} & \tau_{0,y} & \tau_{0,z} & \tau_1 & \tau_2 \end{bmatrix}^\top \quad (8)$$

Note that the thruster forces could also easily be written in ${}^I\mathcal{F}$ via a frame transformation. For this scenario, \mathbf{H} has the following form:

$$\mathbf{H}(\mathbf{q}) = \begin{bmatrix} M\mathbf{I}_{3 \times 3} & \mathbf{M}_{r\omega} & \mathbf{M}_{rm} \\ \mathbf{M}_{r\omega}^\top & \mathbf{M}_\omega & \mathbf{M}_{\omega m} \\ \mathbf{M}_{rm}^\top & \mathbf{M}_{\omega m}^\top & \mathbf{M}_m \end{bmatrix} \quad (9)$$

M is the total system mass, $\mathbf{M}_\omega \in \mathbb{R}^{3 \times 3}$ captures base rotation affecting ω , $\mathbf{M}_{\omega m} \in \mathbb{R}^{3 \times n}$ is a coupling term that shows the effect of arm motion on base attitude disturbance and $\mathbf{M}_m \in \mathbb{R}^{n \times n}$ captures the self-disturbance of the arm. The remaining terms are due to using the satellite base CM, rather than the system CM. Alternatively, the entire dynamics can be summarized in the robot manipulator format of equation 10, with terms grouped to explicitly represent impacts on the base, ‘0’, and on the manipulator, ‘m’. An additional \mathbf{B} matrix is listed for mixing thruster outputs into force and torque commands, though it is not needed for this scenario.

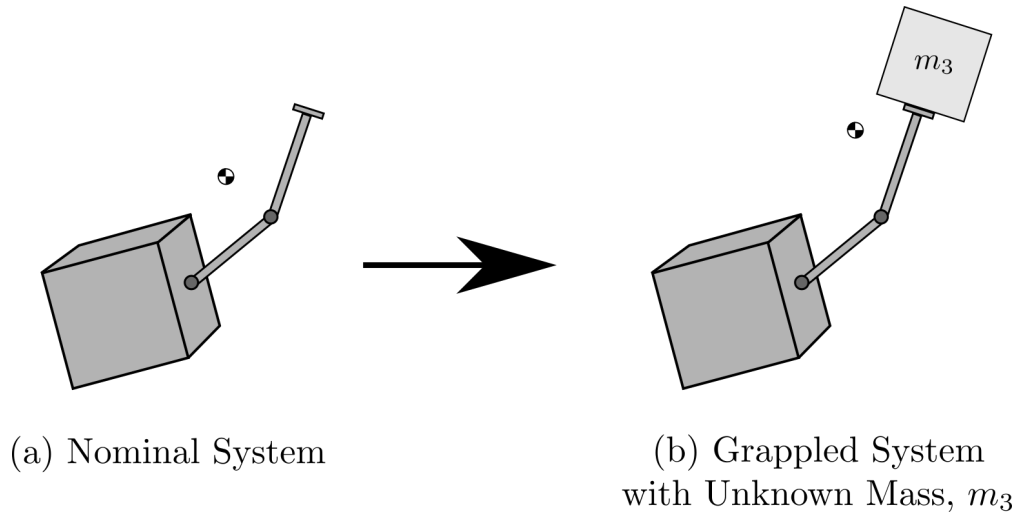


Fig. 3 Introduction of Parametric Uncertainty. In (a), the nominal system has known parameters and a finely-tuned deterministic controller may be developed. In (b), the system has grappled a payload of unknown mass, adding an unknown parameter to the model, m_3 . The nominal system model has surely changed.

A grappling scenario is considered, where some target has been grappled by the free-flyer and must be transported following some reference trajectory, \mathbf{r}_{des} and its first and second derivatives. This results in uncertainty in equation 10,

namely in the parameters involving the end effector. For simplicity and as a proof-of-concept, this formulation will consider a grappled *point mass*, meaning that there is a single unknown parameter, m_3 , the mass of the grappled point mass payload perched exactly on the end of link 2. Fig. 3 shows this scenario, where the payload in (b) can be thought of as a point mass.

$$\begin{bmatrix} \mathbf{M}_0 & \mathbf{M}_{0m} \\ \mathbf{M}_{0m}^\top & \mathbf{M}_m \end{bmatrix} \begin{bmatrix} \ddot{\mathbf{q}}_0 \\ \ddot{\mathbf{q}}_m \end{bmatrix} + \begin{bmatrix} \mathbf{C}_0 & \mathbf{C}_{0m} \\ \mathbf{C}_{0m}^\top & \mathbf{C}_m \end{bmatrix} \begin{bmatrix} \dot{\mathbf{q}}_0 \\ \dot{\mathbf{q}}_m \end{bmatrix} = \begin{bmatrix} \boldsymbol{\tau}_0 \\ \boldsymbol{\tau}_m \end{bmatrix} + \begin{bmatrix} \mathbf{B}_0 & \mathbf{B}_{0m} \\ \mathbf{B}_{0m}^\top & \mathbf{B}_m \end{bmatrix} \begin{bmatrix} \mathbf{u}_0 \\ \mathbf{u}_m \end{bmatrix} \quad (10)$$

IV. Approach

A common control approach for AFFs is simple PD position control [18]. For trajectory control, feedback linearization is another commonly-cited option in the traditional free-flyer literature [3]. However adaptive control is particularly appealing because of the non-varying parametric uncertainty of this problem. (See Chapter 9 of Slotine and Li for a similar description for fixed-based manipulators [19].) A sliding mode adaptive controller formed specifically for the free-flying dynamics will be presented and compared to other control methods. Each controller is discussed in turn: Subsection IV.A discusses *PD Control*, Subsection IV.B discusses *Feedback Linearization*, and Subsection IV.C presents *Adaptive Control*.

A. Proportional-Derivative (PD) Control

PD control aims to achieve a specified state vector using feedback on the system positions and velocities. Essentially, the system can be thought to have “virtual springs and dampers” that adjust its dynamics tune-ably based on the gain values and state reference. PD control is often simple to implement but lacks optimal tracking performance [19]. For this system, a position controller of the form below may be used:

$$\boldsymbol{\tau} = -\mathbf{K}_p \mathbf{r}_{err} - \mathbf{K}_d \mathbf{v}_{err} \quad (11)$$

Note that this is a modification from pure position control, since the reference trajectory of \mathbf{v}_{des} may be non-zero.

B. Feedback Linearization Trajectory Control

Building on PD control, it is possible to achieve better tracking performance if a control law respecting a trajectory (containing one derivative beyond the state vector) is produced. For nonlinear systems, this is often accomplished via feedback linearization such that system accelerations follow ones prescribed. However, this assumes exact knowledge of the dynamics.

Again following from Slotine and Li [19] and using the manipulator equations of equation 6 and rearranging, a trajectory control strategy can be produced via:

$$\boldsymbol{\tau} = \mathbf{C}\mathbf{v} + \mathbf{H}[-\lambda^2 \mathbf{r}_{err} - 2\lambda \mathbf{v}_{err} + \dot{\mathbf{v}}_{des}] \quad (12)$$

This control effectively cancels the model of the system dynamics, allowing a desired reference trajectory to be specified directly. Note that a reference acceleration must be designated via this procedure, $\dot{\mathbf{v}}_{des}$. The gain matrix may be tweaked as before for desired system performance.

C. Adaptive Control

If knowledge of the dynamics is not exact then adaptive and/or robust control methods become appealing. Reference-tracking control with guarantees on performance are desirable—adaptive control, which uses sliding mode control to adapt parameters online and converge to a sliding surface is appropriate for the parametric uncertainty of this problem formulation. Previous investigations using adaptive control have been demonstrated for both rigid and flexible link manipulators with low payload mass fraction [20] [21], and for the general free-floating dynamics under various

assumptions [10] [11] [12]. However, work by Senda et al. first adapted some of the developments by Slotine and Li to free-flying adaptive control, including base control [13]. Notably, other interesting and more recent approaches consider e.g., multiple arms or other control methods [14].

Senda's approach uses an adaptive control approach based directly on Slotine's fixed-base adaptive controller, which relies on a linear parameterization of the dynamics in terms of the adaptation parameters [19]. However, the free-flying dynamics are more complicated and higher-dimensional than those of fixed-base dynamics, so determining reasonable parameterizations is extremely challenging. An adaptive controller similar to Senda's and the generic manipulator equation formulation of Slotine and Li is presented here, with additional clarification about the parameterization used. For this case, the uncertain parameter vector, \mathbf{a} is simply a scalar:

$$a = [m_3] \quad (13)$$

An adaptation and control law must be produced so that the unknown parameters can be tweaked during operation and so control inputs can be determined. For a second order system, a sliding variable \mathbf{s} is introduced:

$$\mathbf{s} = \mathbf{v}_{err} + 2\lambda_0 \mathbf{r}_{err} \quad (14)$$

where λ_0 is used to define convergence on the sliding surface. Reference values of $\dot{\mathbf{v}}_r$ and \mathbf{v}_r are produced according to the desired trajectory and current tracking error:

$$\dot{\mathbf{v}}_r = \dot{\mathbf{v}}_{des} - 2\lambda_0 \dot{\mathbf{e}} \quad (15)$$

$$\mathbf{v}_r = \mathbf{v}_{des} - 2\lambda_0 \dot{\mathbf{e}} \quad (16)$$

The next step is choosing a set of parameters—perhaps more complex than the actual underlying uncertain parameter(s)—that can be linearly combined with nonlinear functions to produce $\dot{\mathbf{v}}$. For the two-link sixteen-dimensional nonlinear system, this is a real challenge. Senda et al. claim that the free-flying dynamics can be affinely parameterized in terms of the unknown parameters, \mathbf{a} . A \mathbf{Y} matrix for adaptation is formed, grouping all terms appearing linearly with \mathbf{a} . Additionally, a state-varying matrix $\mathbf{Q}(\mathbf{q})$ appears for the free-flying dynamics and must be accounted for, shown in equation 17:

$$\mathbf{H}(\mathbf{q})\dot{\mathbf{v}}_r + \mathbf{C}(\mathbf{q}, \omega_0, \dot{\mathbf{q}})\mathbf{v}_r = \mathbf{Y}(\mathbf{r}, \mathbf{v}, \mathbf{v}_r, \dot{\mathbf{v}}_r)\mathbf{a} + \mathbf{Q}(\mathbf{q}) \quad (17)$$

Since this controller differs slightly from traditional fixed-manipulator linear parameterizations (i.e., without a $\mathbf{Q}(\mathbf{q})$), a Lyapunov-based proof of reference-tracking convergence is provided here, following closely the steps in Slotine and Li [19]. The control and adaptation laws are introduced in the course of the proof.

A candidate Lyapunov function is defined:

$$V = \frac{1}{2} \mathbf{s}^\top \mathbf{H}(\mathbf{q}) \mathbf{s} + \frac{1}{2} \tilde{a}^\top \Gamma^{-1} \tilde{a} \quad (18)$$

where $\tilde{a} = \hat{a} - a$ is the parameter error. Differentiating the candidate Lyapunov function yields

$$\dot{V} = \mathbf{s}^\top (\mathbf{H}\dot{\mathbf{s}}) + \frac{1}{2} \mathbf{s}^\top \dot{\mathbf{H}}(\mathbf{q}) \mathbf{s} + \dot{\hat{a}}^\top \Gamma^{-1} \tilde{a} \quad (19)$$

$$= \mathbf{s}^\top (\mathbf{H}\dot{\mathbf{v}} - \mathbf{H}\dot{\mathbf{v}}_r) + \frac{1}{2} \mathbf{s}^\top \dot{\mathbf{H}}(\mathbf{q}) \mathbf{s} + \dot{\hat{a}}^\top \Gamma^{-1} \tilde{a} \quad (20)$$

where the fact that the parameter error rate $\dot{\tilde{a}} = \dot{\hat{a}}$ is used. Substituting the dynamics in equation 6, and noting that $\mathbf{v} = \mathbf{s} + \mathbf{v}_r$ yields:

$$\dot{V} = \mathbf{s}^\top (-\mathbf{C}(\mathbf{q}, \omega_0, \dot{\mathbf{q}}) (\mathbf{s} + \mathbf{v}_r) + \boldsymbol{\tau} - \mathbf{H}(\mathbf{q})\dot{\mathbf{v}}_r) + \frac{1}{2} \mathbf{s}^\top \dot{\mathbf{H}}(\mathbf{q}) \mathbf{s} + \dot{\hat{a}}^\top \Gamma^{-1} \tilde{a} \quad (21)$$

For many mechanical systems, including the free-flying dynamics, the matrix $\mathbf{H} - 2\mathbf{C}$ is skew-symmetric. Therefore, it is possible to simplify the expression of \dot{V} as:

$$\dot{V} = \mathbf{s}^\top (-\mathbf{H}(\mathbf{q})\dot{\mathbf{v}}_r - \mathbf{C}(\mathbf{q}, \omega_0, \dot{\mathbf{q}})\mathbf{v}_r + \boldsymbol{\tau}) + \dot{\hat{\mathbf{a}}}^\top \Gamma^{-1} \tilde{\mathbf{a}} \quad (22)$$

$$= \mathbf{s}^\top (-\mathbf{Y}(\mathbf{r}, \mathbf{v}, \mathbf{v}_r, \dot{\mathbf{v}}_r)\mathbf{a} - \mathbf{Q}(\mathbf{q}) + \boldsymbol{\tau}) + \dot{\hat{\mathbf{a}}}^\top \Gamma^{-1} \tilde{\mathbf{a}} \quad (23)$$

The control is chosen to be:

$$\boldsymbol{\tau} = \mathbf{Y}(\mathbf{r}, \mathbf{v}, \mathbf{v}_r, \dot{\mathbf{v}}_r)\hat{\mathbf{a}} + \mathbf{Q}(\mathbf{q}) - \mathbf{K}_D \mathbf{s} \quad (24)$$

where \mathbf{K}_D is a positive definite matrix. Furthermore, the adaptation law is selected as:

$$\dot{\hat{\mathbf{a}}} = -\Gamma \mathbf{Y}(\mathbf{r}, \mathbf{v}, \mathbf{v}_r, \dot{\mathbf{v}}_r)^\top \mathbf{s} \quad (25)$$

where Γ is a positive constant that influences adaptation rate. The time derivative of the Lyapunov function then becomes:

$$\dot{V} = \mathbf{s}^\top (\mathbf{Y}(\mathbf{r}, \mathbf{v}, \mathbf{v}_r, \dot{\mathbf{v}}_r)\tilde{\mathbf{a}} - \mathbf{K}_D \mathbf{s}) + \dot{\hat{\mathbf{a}}}^\top \Gamma^{-1} \tilde{\mathbf{a}} \quad (26)$$

$$= -\mathbf{s}^\top \mathbf{K}_D \mathbf{s} \leq 0 \quad (27)$$

By Barbalat's Lemma, it can be shown that $\mathbf{s} \rightarrow 0$, which implies $\mathbf{v}_{err} \rightarrow 0$, $\dot{\mathbf{v}}_{err} \rightarrow 0$. Therefore, the control law in equation (24) and adaptation law in equation (25) ensure convergence to the reference signal.

V. Results

The free-flying manipulator dynamics were implemented in MATLAB, using a wrapped version of the Spacecraft Robotics Toolkit (SPART) for the forward dynamics [17]. SPART uses an internal solver to more efficiently solve for the forward dynamics of multi-link systems than via equation 6, but requires careful interfacing to maintain coordinate conventions and state updating. MATLAB's ODE23 numerical integration tool was used for system propagation; the reference trajectory and adaptive tracking controller were integrated into this framework.

Reference trajectories were created for (1) a simple step response (Step), (2) a more complex base movement with an arm swing called the AFF trajectory, and (3) a persistent excitation state movement called PE. The AFF trajectory is representative of the faster, more complex maneuvers that are expected to become commonplace for AFFs—this example might be representative of placing a grappled object in a desired location on a cluttered space station, for instance. The AFF trajectory's position component is shown in Fig. 4. The PE trajectory consisted of a random integer value signal similar to that of a pseudo-random binary sequence.

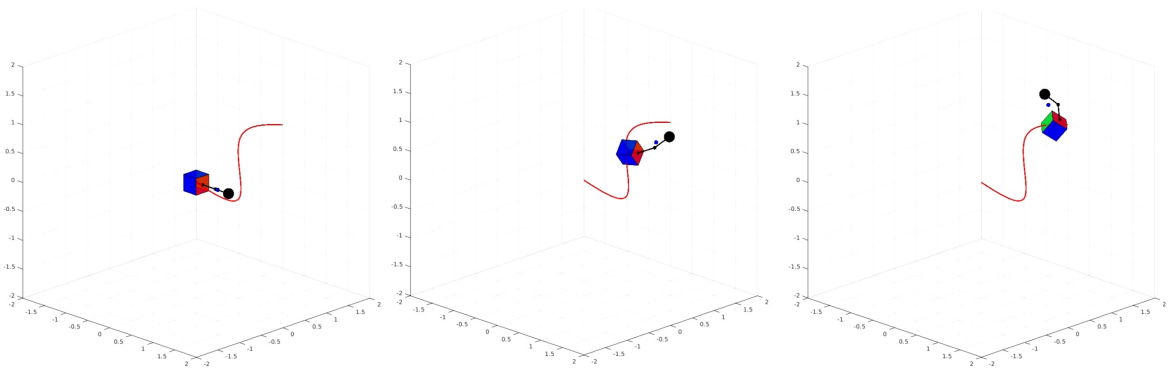


Fig. 4 The AFF Trajectory. The cube represents the spacecraft base, the large black ball is the end effector, and the blue ball is the system CM position. Trajectories of this sort, involving significant “quick” base repositioning are seldom found in existing literature for free-flyers.

The full trajectories for Step and AFF were obtained using simple finite differencing of the prescribed position commands (a fairly rough approximation for the true Euler angle rates), while the PE trajectory was obtained by integrating the input excitation. First, the PE and AFF trajectories were tracked using adaptive control in order to demonstrate mass adaptation and the role of persistent excitation. Next, the Step and AFF trajectories were tested with tuned versions of the aforementioned controllers with exact system knowledge. Then, the Step and AFF trajectories were tested with modified end effector mass due to grappling an object: these modified properties were not known beforehand, so gains (and parameter estimates) are unchanged initially. The system performance was evaluated over a range of mass fractions, γ , for these controllers:

$$\gamma = \frac{m_3}{M + m_3} \quad (28)$$

M indicates the system mass before grappling and m_3 is the unknown mass parameter which has modified the nominal system. The reference trajectories are made “sufficiently fast” so that model error and nonlinearity becomes significant in system performance. The experimental system parameters are provided in Table 1.

Parameter	Default System	Grappled System
m_0 [kg]	10.0	-
I_0 [kg-m ²]	0.1	-
$l_{0,x}$ [m]	0.145	-
$r_{CM,1}$ [m]	0.15	-
m_1 [kg]	1.0	-
I_1 [kg-m ²]	0.05	-
$l_{1,x}$ [m]	0.3	-
$r_{CM,2}$ [m]	0.15	-
m_2 [kg]	1.0	-
I_2 [kg-m ²]	0.05	-
$l_{2,x}$ [m]	0.3	-
$r_{CM,3}$ [m]	0.0	-
m_3 [kg]	0.0	0.0-20.0 (unknown)
I_3 [kg-m ²]	0.0	-

Table 1 System Parameter Values. I_0 represents moment of inertia, which is set to be spherical ($I_{xx} = I_{yy} = I_{zz}$). $r_{CM,*}$ values are with respect to the prior link body frame, in the x direction.

A. Controller Definition and the Role of Adaptation

The PD and feedback linearization controllers were tuned for the nominal case, with perfect knowledge of the system parameters. The following gains were used:

$$\mathbf{K}_p = \begin{bmatrix} 30.0 & 0 & \dots & & \dots & 0 \\ 0 & 30.0 & & & \ddots & \vdots \\ \vdots & & 30.0 & & & \\ & & & 0.1 & & \\ & & & & 0.1 & \\ & & & & & 0.1 & \vdots \\ \vdots & \ddots & & & & 1.5 & 0 \\ 0 & \dots & & \dots & 0 & 1.5 \end{bmatrix}$$

$$\mathbf{K}_d = 5.0 * \mathbf{I}_{8 \times 8}$$

$$\lambda = \begin{bmatrix} 1.0 & 0 & \dots & & \dots & 0 \\ 0 & 1.0 & & & \ddots & \vdots \\ \vdots & & 1.0 & & & \\ & & & 2.0 & & \\ & & & & 2.0 & \\ & & & & & 2.0 & \vdots \\ \vdots & \ddots & & & & 2.0 & 0 \\ 0 & \dots & & \dots & 0 & 2.0 \end{bmatrix}$$

Neither PD control nor feedback linearization are able to account for system parameter changes. Cancellation of nonlinearity using a perfect system model allows feedback linearization to achieve better tracking performance than PD control in practice, but this performance can easily degrade with model inaccuracy. The adaptive controller presented earlier, however, has the ability to actively compensate for the change in mass. As a result, mass adaptation was observed during runs on sample trajectories AFF and PE, as demonstrated in Fig. 5 for $m_3 = 8.0$ kg. Values of $\Gamma = 500.0$, $\lambda_0 = 1.0$ and $\mathbf{K}_D = \mathbf{I}_{8 \times 8}$ were used for simplicity.

Fig. 5 also shows the benefit of having an input that has persistent excitation compared to the AFF trajectory. It is well known that if the desired trajectory being followed by an adaptive controller meets a “persistent excitation” condition, then the estimated parameter will converge to the true parameter [19]. This behavior is observed in the PE reference trajectory, where parameter convergence is faster than that seen for the AFF trajectory. This yields an interesting problem of the trade-offs of designing a trajectory that enhances parameter estimation while simultaneously accomplishing useful motion [22].

B. Tracking Performance with Increasing Mass Fraction

An analysis was performed to determine the effect of the unknown payload mass on adaptive and non-adaptive controllers. For this analysis, the unknown payload mass was varied from 0 to 20 [kg], effectively changing the payload to system mass fraction, γ , from 0 to 0.625.

Figs. 6a and 6b show the position and angular root-mean-squared (RMS) error between two candidate trajectories for the controllers. For all mass fraction values, the PD controller has worse tracking performance than the adaptive controller; the feedback linearization controller has superior position performance on AFF for low mass fraction values, with a worsening decline in performance as mass fraction increases. The AFF trajectory, a richer and more challenging signal than the Step trajectory, leads to even worse performance in the PD controller that is exacerbated with greater γ . For example, the rate of change in the increase of position RMS error for the PD controller following the AFF trajectory is higher than that of the Step trajectory as shown in Fig. 6a; feedback linearization show a similar trend. It is important to note that these results reveal performance for a specific set of gain values—tuning gains for both the adaptive and non-adaptive controllers is a project unto itself. So, for low (or 0) mass fraction values it is entirely plausible that a

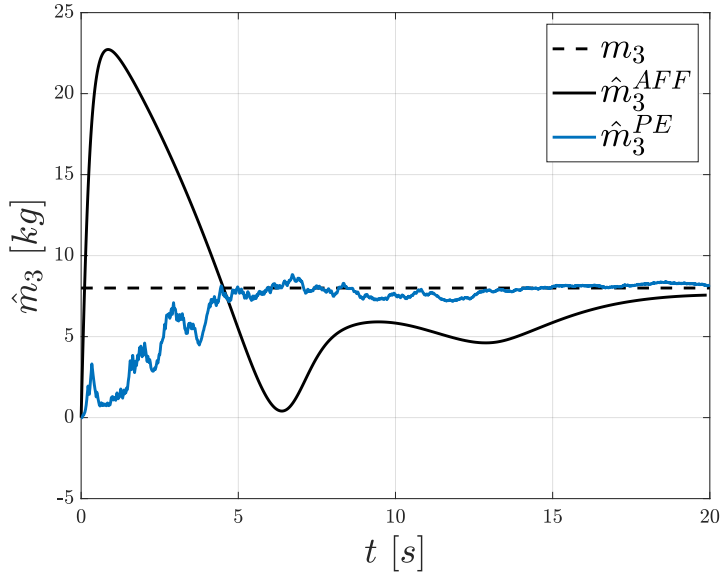


Fig. 5 Adaptation of m_3 for the AFF and PE Trajectories for $m_3 = 8.0$ [kg].

non-adaptive controller might have superior tracking performance to an adaptive controller for a particular set of gains; the important trend to note is the decline in RMS performance as mass fraction increases, which is far more severe for the non-adaptive approaches as expected.

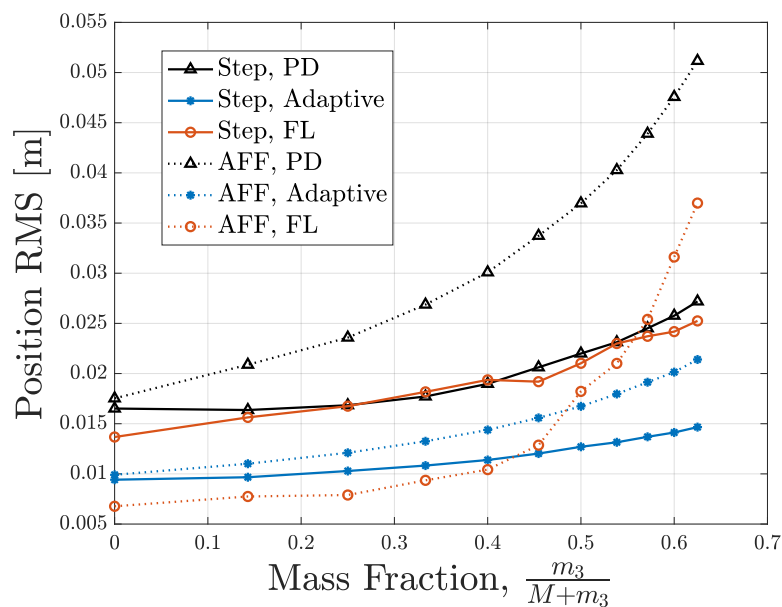
Additionally the total RMS error was computed for a sample case in which the payload mass is $m_3 = 10$ [kg] but the initial model system knowledge is $\hat{m}_3 = 0$ [kg]. The results for all three reference trajectories are shown in Table 2. The total RMS is a measure of the total error for both positions and velocities and is computed as $\sum_i \sum_j (\mathbf{x}_j(t_i) - \mathbf{x}_{j,des}(t_i))^2$. Again, the total RMS error for the adaptive controller is significantly smaller than that of the PD and feedback linearization controllers.

Metric	Step			AFF			PE		
	PD	FL	Adaptive	PD	FL	Adaptive	PD	FL	Adaptive
Total RMS	0.137	0.287	0.036	0.208	0.327	0.048	0.223	0.369	0.026

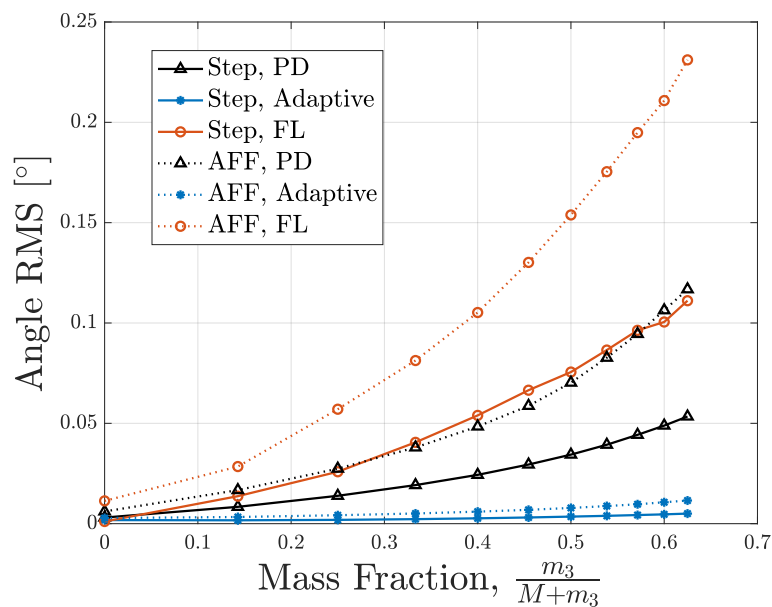
Table 2 Total RMS Error for the Adaptive and Non-Adaptive Controllers for an Unknown 10 [kg] Payload.

VI. Conclusions

This paper has shown the free-flying dynamics for a six DoF base two-link manipulator system and set up the grappling problem, where system mass parameters change after a payload has been acquired. This scenario is reflective of future scenarios involving AFF operation. Adaptive control is introduced as a solution, and compared against PD control and feedback linearization, both common non-adaptive control approaches. The unique Lyapunov parameterization and Lyapunov analysis for this system is introduced to show tracking convergence of the adaptive controller. The controllers were demonstrated on a standard step reference trajectory (Step), and a more complex trajectory called the AFF trajectory over a range of grappled payload mass values. The AFF trajectory was also compared to a persistent excitation trajectory for the adaptive controller to demonstrate the effect of excitation on parameter convergence. This case study is a step toward developing control and planning methods that will account for the structured parametric uncertainties AFFs will see on-orbit, and demonstrates a unique adaptive control method for these free-flying systems; the benefit in terms of tracking performance is clearly demonstrated. Code for this case study is available on [GitHub](#).



(a) Average Position RMS for the Adaptive and Non-Adaptive Controllers Tracking Step and AFF Trajectories.



(b) Average Angular RMS for the Adaptive and Non-Adaptive Controllers Tracking Step and AFF Trajectories.

Fig. 6 Effect of Unknown Payload Mass on Controller Performance. Adaptive controller performance is better in both the angular and position error RMS for both the Step and AFF trajectories, particularly for higher mass fractions.

Acknowledgements

The authors would like to thank Prof. Jean-Jacques Slotine and Carlos Barajas for their work in teaching 2.152 at MIT, which influenced the development of this paper. A portion of this work was sponsored by the NASA Space Technology Mission Directorate through a NASA Space Technology Research Fellowship under grant 80NSSC17K0077. Additionally, a portion of this material is based upon work supported by the National Science Foundation Graduate Research Fellowship under grant number 1745302. The authors gratefully acknowledge the support that enabled this research.

References

- [1] Smith, T., Barlow, J., Bualat, M., Fong, T., Provencher, C., Sanchez, H., and Smith, E., "Astrobee: A New Platform for Free-Flying Robotics on the ISS," Tech. rep., 2016.
- [2] Saenz-Otero, A., and Miller, D. W., "Design Principles for the Development of Space Technology Maturation Laboratories Aboard the International Space Station," Ph.D. thesis, MIT, 2005.
- [3] Dubowsky, S., and Papadopoulos, E., "The Kinematics, Dynamics, and Control of Free-Flying and Free-Floating Space Robotic Systems," *IEEE Transactions on Robotics and Automation*, 1993. <https://doi.org/10.1109/70.258046>.
- [4] Yoshida, K., Hashizume, K., and Abiko, S., "Zero Reaction Maneuver: Flight Validation with ETS-VII Space Robot and Extension to Kinematically Redundant Arm," *IEEE International Conference on Robotics and Automation*, 2001, pp. 441–446.
- [5] Estrada, M. A., Hockman, B., Bylard, A., Hawkes, E. W., Cutkosky, M. R., and Pavone, M., "Free-flyer acquisition of spinning objects with gecko-inspired adhesives," *Proceedings - IEEE International Conference on Robotics and Automation*, Vol. 2016-June, 2016, pp. 4907–4913. <https://doi.org/10.1109/ICRA.2016.7487696>.
- [6] Fong, T., Micire, M., Morse, T., Park, E., Provencher, C., To, V., Wheeler, D., Mittman, D., Torres, R. J., and Smith, E., "Smart SPHERES: a Telerobotic Free-Flyer for Intravehicular Activities in Space," *AIAA SPACE Conference*, 2013. URL <https://ntrs.nasa.gov/archive/nasa/casi.ntrs.nasa.gov/20160006694.pdf>.
- [7] Papadopoulos, E., "On the Dynamics and Control of Space Manipulators," Ph.D. thesis, MIT, 1990.
- [8] Papadopoulos, E., and Dubowsky, S., "Dynamic Singularities in Free- Floating Space Manipulators," *Journal of Dynamic Systems, Measurement and Control*, Vol. 115, No. 1, 1993, pp. 44–52.
- [9] Xu, Y., and Kanade, T., *Space Robotics: Dynamics and Control*, Springer Science+Business Media, New York, 1993.
- [10] Walker, M., and Wee, L.-B., "Adaptive Control of Space Based Robot Manipulators," Tech. rep., 1991. <https://doi.org/10.1017/CBO9781107415324.004>.
- [11] Shin, J. H., Jeong, I. K., Lee, J. J., and Ham, W., "Adaptive robust control for free-flying space robots using norm-bounded property of uncertainty," *IEEE International Conference on Intelligent Robots and Systems*, Vol. 2, 1995, pp. 59–63. <https://doi.org/10.1109/iros.1995.526139>.
- [12] Gu, Y. L., and Xu, Y., "A normal form augmentation approach to adaptive control of space robot systems," *Dynamics and Control*, Vol. 5, No. 3, 1995, pp. 275–294. <https://doi.org/10.1007/BF01968678>.
- [13] Senda, K., Nagaoka, H., and Murotsu, Y., "Adaptive control of free-flying space robot with position/attitude control system," *Journal of Guidance, Control, and Dynamics*, Vol. 22, No. 3, 1999, pp. 488–490. <https://doi.org/10.2514/2.7630>.
- [14] Jia, Y.-H., Hu, Q., and Xu, S., "Dynamics and adaptive control of a dual-arm space robot with closed-loop constraints and uncertain inertial parameters," *Acta Mechanica Sinica*, Vol. 30, No. 1, 2014, pp. 112–124. <https://doi.org/10.1007/s10409-014-0005-1>.
- [15] Lampariello, R., and Hirzinger, G., "Identification of Free-Flying Space Robots," 2005.
- [16] Jayakody, H. S., Shi, L., Katupitiya, J., and Kinkaid, N., "Robust adaptive coordination controller for a spacecraft equipped with a robotic manipulator," *Journal of Guidance, Control, and Dynamics*, Vol. 39, No. 12, 2016, pp. 2699–2711. <https://doi.org/10.2514/1.G002145>.
- [17] Virgili-Llop, J., Drew Ii, J. V., and Romano, M., "Spacecraft Robotics Toolkit: An Open-Source Simulator for Spacecraft Robotic Arm Dynamic Modeling and Control," 2017. URL <https://indico.esa.int/indico/event/111/session/38/contribution/76/material/paper/0.pdf>.
- [18] Flückiger, L., Browne, K., Coltin, B., Fusco, J., Morse, T., and Symington, A., "Astrobee Robot Software: Enabling Mobile Autonomy on the ISS," Tech. rep., 2018.
- [19] Slotine, J.-J. E., and Li, W., "On the Adaptive Control of Robot Manipulators," 1986. URL <http://journals.sagepub.com/doi/pdf/10.1177/027836498700600303>.
- [20] Ulrich, S., and Sasiadek, J. Z., "Modified Simple Adaptive Control for a Two-Link Space Robot," *Proceedings of the 2010 American Control Conference, ACC 2010*, 2010, pp. 3654–3659. <https://doi.org/10.1109/acc.2010.5530518>.
- [21] Ulrich, S., Sasiadek, J. Z., and Barkana, I., "Modeling and direct adaptive control of a flexible-joint manipulator," *Journal of Guidance, Control, and Dynamics*, Vol. 35, No. 1, 2012, pp. 25–39. <https://doi.org/10.2514/1.54083>.

- [22] Albee, K., Ekal, M., Ventura, R., and Linares, R., “Combining Parameter Identification and Trajectory Optimization: Real-Time Planning for Information Gain,” *ESA Advanced Space Technologies for Robotics and Automation (ASTRA)*, Noordwijk, The Netherlands, 2019.